RSC Applied Polymers

ROYAL SOCIETY OF CHEMISTRY

PAPER

View Article Online
View Journal | View Issue

Cite this: *RSC Appl. Polym.*, 2025, **3**, 163

Reprocessable, recyclable and shape programmable epoxy vitrimers†

Hongxin Yao,[a] Hongjun Yang, *[b] Li Jiang, [b] Wenyan Huang,[b] Qimin Jiang,[b] Bibiao Jiang [b] and Guangzhao Zhang [a]

Received 1st July 2024,
Accepted 30th October 2024

DOI: 10.1039/d4lp00216d

rsc.li/rscapplpolym

Epoxy vitrimers are versatile thermoset polymers with good mechanical and reprocessable properties. Generally, they are prepared with complex procedures by using petroleum-based monomers. Herein, we report a one-pot catalyst-free procedure to synthesize bio-based epoxy vitrimers. Diacrylate was used to react with amine *via* aza-Michael addition yielding β-amino esters with reversible dynamic covalent bonds which can be strengthened by the *in situ* generated tertiary amine groups. Because of the ester and β-amino esters, the bio-based epoxy vitrimers can be reprocessed and readily programmed. Moreover, due to the introduced ester group from diacrylate, the produced epoxy vitrimer showed good recyclability. This study provides a feasible strategy to develop intelligent materials based on epoxy vitrimers.

Introduction

As one of the most important thermosetting materials, epoxy resins exhibit good mechanical properties, excellent thermal stability and high durability.[1–5] They have found applications in adhesives, composites, electronic packaging and other fields.[6–10] Yet, most of the thermosetting epoxy resins are neither degradable nor recyclable due to their chemically cross-linked nature.[11–13] Actually, great efforts have been made to synthesize recyclable epoxy vitrimers based on dynamic covalent chemistry, where the crosslinked networks can reversibly rearrange.[14–18]

Leibler *et al.*[19] first reported recyclable epoxy/acid or epoxy/anhydride polyester networks with transesterification catalysts. Afterwards, many exchange reactions including disulfide exchange,[20–23] imide bond exchange,[24–26] boronic ester exchange,[27–30] and Diels–Alder reactions[31–33] were used to develop recycled epoxy, wherein transesterification reaction has gained particular interest because the resulting epoxy vitrimer can be degraded into a monomer or useful oligomer.[34–39] However, a large amount of catalyst had to be used to promote the exchange reaction between dynamic covalent bonds.[40–42] Such an epoxy vitrimer exhibits poor mechanical properties because of the poor compatibility between the matrix resin and catalysts if the latter are not removed. Moreover, the catalysts would significantly decrease the thermostability of the vitrimer. To solve the problem, catalyst-free synthesis of epoxy vitrimers was developed. Ladmiral *et al.*[43] reported such a vitrimer based on transesterification internally activated by the α-CF_3 group. Zhang *et al.*[44] prepared the vitrimers by using a self-catalytic monomer. The catalyst-free epoxy vitrimers show much improved mechanical properties. On the other hand, most of the epoxy resins are made from non-renewable fossil resources. As biomass is the most abundant renewable resource on Earth, it is highly desirable to develop epoxy vitrimers based on biomass.[45–50]

In this study, we report a one-pot method for synthesizing vitrimers from a bio-based epoxy, epoxidized soybean oil, where diacrylate is introduced to react with amine *via* aza-Michael addition yielding esters and β-amino ester groups (Scheme 1). This preparation process is exceptionally simple, requiring no addition of solvents or catalysts. Furthermore, the atom economy is nearly 100%, as there are no by-products, and no further purification is necessary. The produced vitrimer has dual dynamic covalent bonds and exhibits good repressibility that can be enhanced by the *in situ* synthesized tertiary amine groups. What's more, the vitrimer can be easily recycled by treatment with alcohol. This work offers a green and economical strategy for epoxy vitrimers and smart materials.

Results and discussion

Synthesis of epoxy vitrimers

For clarity on the polymerization mechanism, we first carried out a model reaction of hexylamine (HA) with methyl acrylate

[a]*Faculty of Materials Science and Engineering, South China University of Technology, Guangzhou 510640, P. R. China*
[b]*Jiangsu Key Laboratory of Environmentally Friendly Polymeric Materials, School of Materials Science and Engineering, Jiangsu Collaborative Innovation Centre of Photovoltaic Science and Engineering, Changzhou University, Changzhou, Jiangsu 213164, P. R. China. E-mail: hjyang0519@cczu.edu.cn*

†Electronic supplementary information (ESI) available. See DOI: https://doi.org/10.1039/d4lp00216d

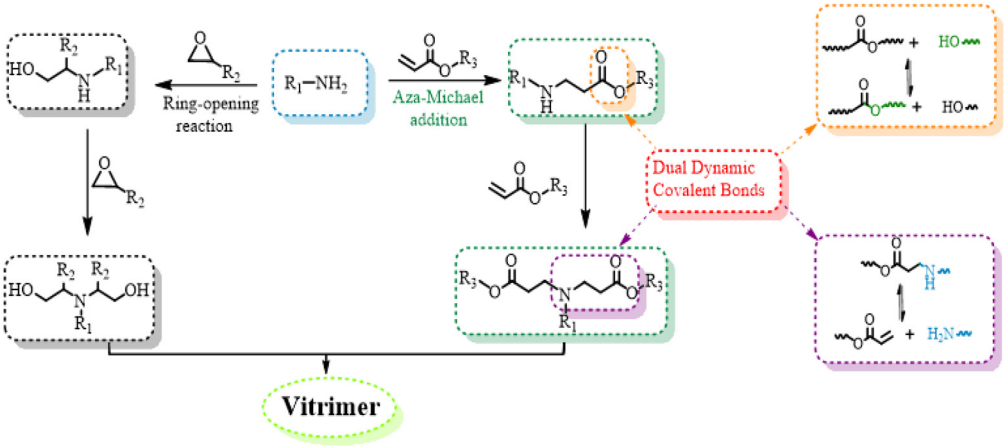

Scheme 1 Mechanism for synthesizing epoxy vitrimers using epoxide, diacrylate and primary amine.

(MA) or/and benzyl glycidyl ether (BGE). The reaction was carried out at 70 °C for 12 hours with a molar ratio of [HA] : [MA] of 1 : 1. No additional catalyst was introduced. Fig. 1a shows the nuclear magnetic resonance (NMR) spectrum of the product from the reaction between HA and MA. The signals at 5.50–6.80 ppm due to the protons of vinyl bonds in MA disappear, and new signals at 2.40–2.50 (c′) and 2.70–2.76 (b′) ppm can be observed due to the formation of methylene groups from the aza-Michael reaction of the primary amine and double bonds. Furthermore, the signals at 2.27–2.37 (c″) and 2.62–2.67 (b″) ppm indicate that the secondary amine could further react with a double bond, producing a tertiary amine as expected.[51–53] After introducing BGE, both the signals due to the ring opening (d′, in Fig. 1b) and the aza-Michael reaction (b′ and c′, in Fig. 1b) can be observed, indicating the completion of the reaction.

A bio-resourced epoxide, epoxidized soybean oil (ESO), was employed to react with 4,4′-methylenedianiline (MDA) and 1,4-butanediol diacrylate (BDDA) for preparing an epoxy vitrimer (Fig. 2). The monomer feed ratio is presented in Table 1. It was fully cured after reacting at 160 °C for 4 h, manifesting the successful synthesis of the thermoset epoxy vitrimer. For comparison, the copolymer (ESO–MDA) of ESO and MDA without BDDA was also prepared.

Fig. 3a illustrates that both ESO–MDA–BDDA and ESO–MDA exhibit high gel fractions (>90%) in common solvents like *n*-hexane, tetrahydrofuran (THF), ethanol (EtOH), dimethyl sulfoxide (DMSO), and water, indicating that they are effectively crosslinked. There is minimal mass loss observed in both EtOH and *n*-hexane, suggesting that the polymers are stable in these solvents. The swelling ratio of ESO–MDA in THF was 311%, and it decreased to 115% for ESO–MDA–BDDA. This indicates that the inclusion of BDDA increases the crosslinking density of the polymer. That is, either ESO–MDA–BDDA or ESO–MDA was crosslinked but the former had much higher crosslink density.

The ESO–MDA–BDDA and monomers were characterized by using FTIR spectra (Fig. 3b). The band assigned to the epoxy groups (829 cm^{-1}) disappeared, whereas a strong and broad band in the range of 3100–3700 cm^{-1} attributed to the hydroxyls after curing was observed for either ESO–MDA–BDDA or ESO–MDA. The facts indicate the successful synthesis

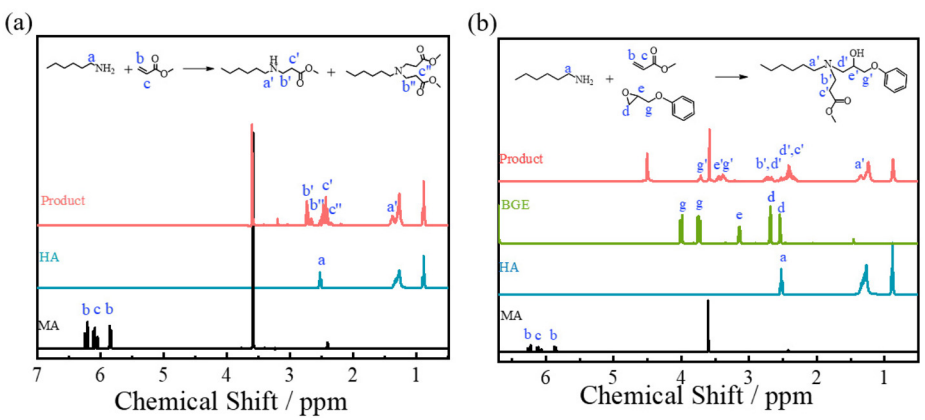

Fig. 1 ^{1}H NMR spectra of the model reactions. (a) [HA]/[MA] = 1/1, at 70 °C for 12 h and (b) [HA]/[MA]/[BGE] = 1/1/1, at 70 °C for 12 h.

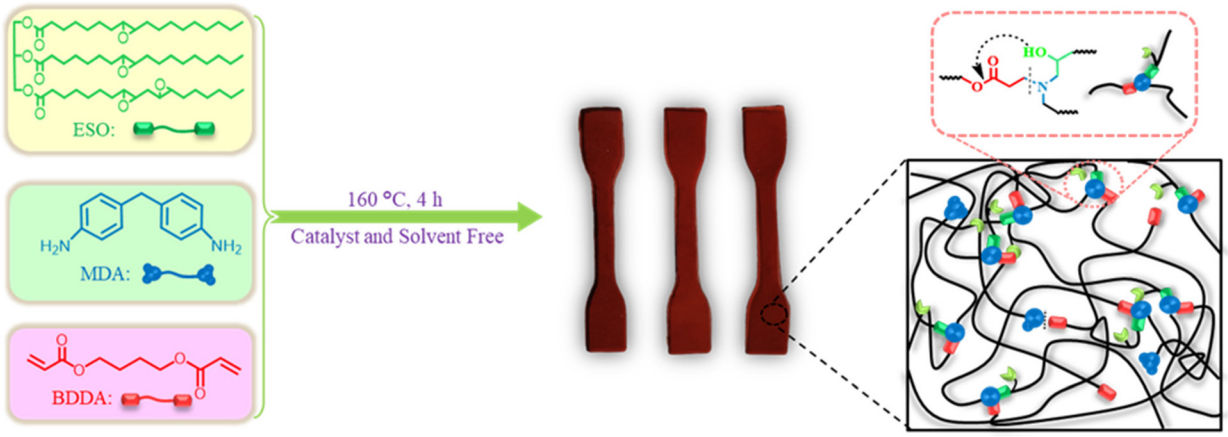

Fig. 2 Synthesis of bio-based epoxy vitrimers.

Table 1 Synthesis of epoxy vitrimers

Sample	ESO/g	EGDE/g	MDA/g	BDDA/g	Time/h	Temp./°C
ESO–MDA	5.00	—	1.52	—	4	160
ESO–MDA–BDDA	5.00	—	3.05	3.04	4	160
EGDE–MDA–BDDA	—	5.00	5.69	5.68	2	130
EGDE–MDA	—	5.00	2.85	—	2	100

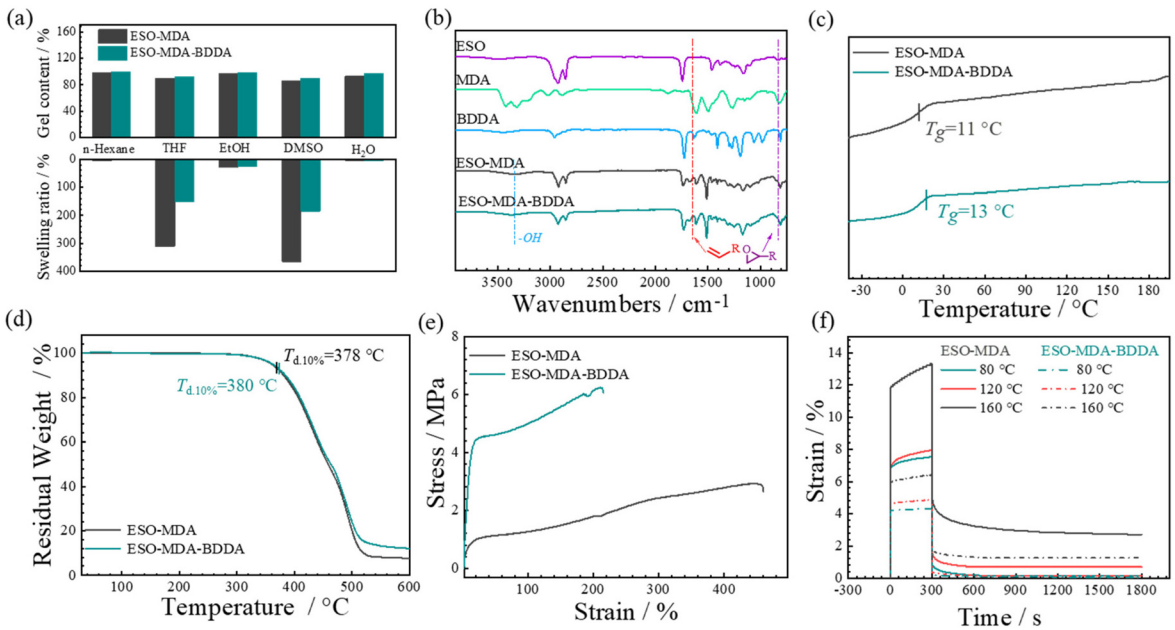

Fig. 3 (a) Swelling ratio and gel content of ESO–MDA–BDDA or ESO–MDA in different solvents; (b) FTIR spectra of ESO, MDA, BDDA, ESO–MDA, and ESO–MDA–BDDA (top to bottom); (c) DSC, (d) TGA, (e) stress–strain, and (f) creep resistance curves of ESO–MDA–BDDA and ESO–MDA.

of the thermoset epoxy. Besides, the bands due to the double bond at 1644 cm^{-1} were no longer observed for ESO–MDA–BDDA, indicating the incorporation of BDDA units into ESO–MDA–BDDA.

Fig. 3c shows the DSC curves of ESO–MDA–BDDA and ESO–MDA. No exotherm was observed for either in the range −50 °C to 200 °C, indicating the completion of the curing reaction. Moreover, ESO–MDA–BDDA had a T_g of ~13 °C, higher

than that of ESO–MDA (11 °C). This is understandable because the former has higher crosslinking density and the mobility of polymer chains is more constrained. The thermal stability of ESO–MDA–BDDA and ESO–MDA was assessed under nitrogen by thermogravimetric analysis as shown in Fig. 3d. The decomposition temperatures at which 10% of the sample mass is lost are 378 °C for ESO–MDA–BDDA and 380 °C for ESO–MDA. These values are higher than the curing temperature, indicating that the vitrimers have good thermal stability during processing.

Fig. 3e shows the stress–strain curves of the vitrimer. ESO–MDA–BDDA exhibited a maximum tensile strength of 6.20 MPa, much higher than that (2.91 MPa) of ESO–MDA. However, the former had a breaking ratio of 213%, significantly lower than that of the latter (456%). This is because of the higher crosslinking density of the former. Fig. 3f shows that ESO–MDA had a deformation of 14% at 80 °C, whereas ESO–MDA–BDDA had a deformation of only 6% at the same temperature. Note that either ESO–MDA–BDDA or ESO–MDA can completely recover from the deformation after removing the stress at a specific temperature. When the temperature was elevated to 160 °C, ESO–MDA had a strain of 12%, much higher than that of ESO–MDA–BDDA (6.5%). After the stress was removed, ESO–MDA and ESO–MDA–BDDA had 4% and 2% permanent deformation, respectively. The irreversible deformation resulted from the rearrangement of ESO–MDA or ESO–MDA–BDDA chains due to dynamic covalent bond exchange, a characteristic of vitrimers.

Dynamic properties

The stress relaxation of ESO–MDA–BDDA or ESO–MDA was investigated at different temperatures by monitoring the reduction in stress as a function of time at a constant strain (5%), where the characteristic relaxation time (τ^*) refers to the time for the relaxation modulus to decrease to $1/e$ of the initial modulus. As shown in Fig. 4a, S1, and S2,† ESO–MDA–BDDA exhibited a shorter τ^* (463 s) than ESO–MDA (836 s) at 200 °C. The dynamic covalent bonds in the former originate from epoxide, BDDA and β-amino esters produced by the aza-Michael reaction, whereas the dynamic covalent bonds in the latter are only from the epoxide. The large number of dynamic covalent bonds in the former accelerated its relaxation, so it had a shorter τ^*. The activation energy (E_a) of the bond exchange was calculated based on the Arrhenius equation (Fig. 4b). ESO–MDA–BDDA had an E_a of 68.69 kJ mol^{-1}, lower than that of ESO–MDA (72.65 kJ mol^{-1}). Thus, ESO–MDA–BDDA with a shorter τ^* and lower E_a is reprocessed more facilely than ESO–MDA.

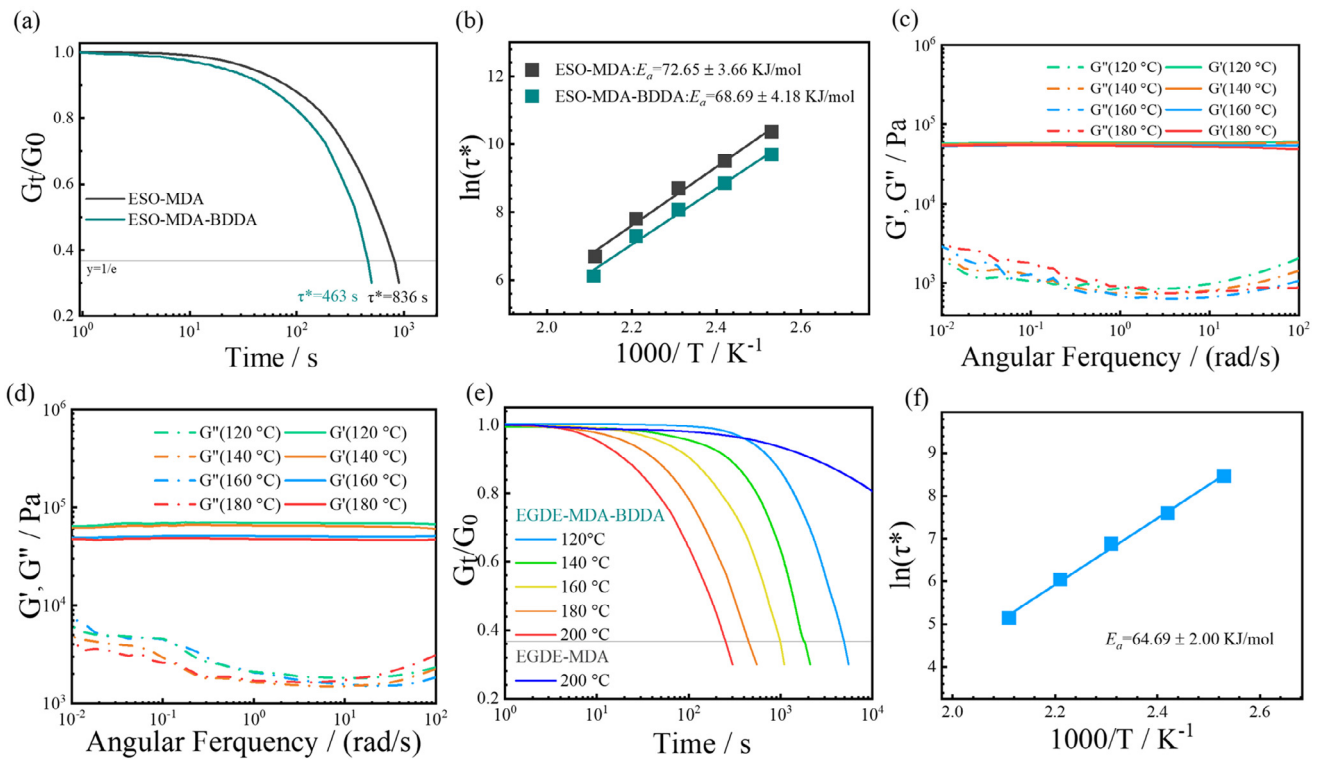

Fig. 4 (a) Normalized stress–relaxation curves of ESO–MDA and ESO–MDA–BDDA; (b) temperature dependence of relaxation time (τ^*) for ESO–MDA and ESO–MDA–BDDA fit by Arrhenius equation; (c) frequency dependence of storage modulus (G') or loss moduli (G'') for ESO–MDA at different temperatures; (d) frequency dependence of storage modulus (G') or loss moduli (G'') for ESO–MDA–BDDA at different temperatures; (e) normalized stress–relaxation curves of EGDE–MDA–BDDA and EGDE–MDA at different temperatures; and (f) temperature dependence of relaxation time (τ^*) for EGDE–MDA–BDDA fit by Arrhenius equation.

As discussed above, the dynamic transesterification and reversible aza-Michael addition are responsible for the stress relaxation of ESO–MDA–BDDA (Fig. 2), where the former follows the associative mechanism but the latter follows the dissociative mechanism. There is an important distinction that can be made between dissociative and associative dynamic networks based on how cross-linking points are (dis) connected as a function of time, resulting in different viscosity profiles. Dissociative covalent adaptable networks (CANs) will show a temporary decrease in network connectivity due to a bond-breaking prior to the formation of a new bond leading to network depolymerization when applying heat. In contrast, associative CANs are characterized by a constant connectivity due to the formation of new cross-linking points before breaking previous ones. In another word, there is only one type of dynamic covalent bond (ester groups) in ESO–MDA.

The dynamic ability of vitrimers was evaluated through frequency sweep experiments conducted with a temperature range of 120–180 °C. Fig. 4c shows that the storage modulus (G') of ESO–MDA slightly decreased from 58.32 kPa at 120 °C to 54.36 kPa at 180 °C, indicating a constant crosslinking density. In contrast, ESO–MDA–BDDA significantly decreased from 68.68 kPa at 120 °C to 46.29 kPa at 180 °C, demonstrating distinct dissociative behaviour. Note that aza-Michael reaction only contributed to the overall dynamic covalent exchange at temperatures above 140 °C and it was negligible at low temperature (<140 °C).[54] Therefore, the dynamic transesterification dominated in ESO–MDA–BDDA.

Actually, ESO–MDA also exhibited the properties of vitrimers due to its ester groups. To further determine the role of ester groups, an ester-free epoxy monomer, ethylene glycol diglycidyl ether (EGDE), was employed to react with MDA. Meanwhile, the copolymer of EGDE with MDA and BDDA was synthesized under the same conditions. As expected, irrespective of the presence of BDDA, it possessed high gel fractions (Fig. S3†), good thermal stability (Fig. S4 and 5†) and good mechanical properties (Fig. S6†). Yet, EGDE–MDA–BDDA could not completely recover from deformation due to the formation of new ester groups after transesterification (Fig. S7†). In contrast, EGDE–MDA did completely recover when the stress was removed (Fig. S8†). EGDE–MDA–BDDA also exhibited excellent stress relaxing properties (Fig. 4e), but EGDE–MDA did not relax in 6 h. On the other hand, EGDE–MDA–BDDA could be reprocessed by hot-pressing, whereas it was not possible for EGDE–MDA. In short, EGDE–MDA–BDDA had characteristics of a typical epoxy vitrimer, but EGDE–MDA did not. The activation energy (E_a) for the bond exchange of EGDE–MDA–BDDA was 64.69 kJ mol^{-1} (Fig. 4f), lower than that of ESO–MDA or ESO–MDA–BDDA. This is because ESO is a trifunctional epoxide monomer, whereas EGDE has two functional epoxide groups. The difference in functionality of the monomers results in the different crosslinking densities in the polymers. Clearly, the introduction of diacrylate to the conditional amine-curing epoxy is an efficient strategy to prepare an epoxy vitrimer.

Reprocessability and recyclability

Unlike general thermoset polymers with permanent cross-linking, an epoxy vitrimer is composed of dynamic covalent bonds which can be regenerated at the appropriate temperature after being broken, so it has good reprocessability. To evaluate the reprocessability, ESO–MDA–BDDA was cut into parts and remolded with three cycles at 160 °C with a pressure of 10 MPa fo2 h. It was homogeneous and transparent after the reprocessing, suggesting that it had good reprocessability. The mechanical and thermal properties of the reprocessed ESO–MDA–BDDA were measured together with those of the original sample. As shown in Fig. 5a, no obvious difference of T_g between the reprocessed and original samples is observed, indicating that the network structure of the vitrimer remains virtually intact in the physical reprocessing.

Fig. 5b shows that the ESO–MDA–BDDA vitrimer had a tensile strength of 6.20 MPa with a break elongation ratio of 213%. After three repressing cycles, the tensile strength decreased to 4.63 MPa and the break elongation ratio increased to 258%. Combining the results from frequency sweep experiments (Fig. 5c) and stress-relaxation (Fig. 5d), we know that the vitrimer can hold more than 70% of the mechanical properties after the reprocessing, so it has good reprocessability. In addition, stress–strain curves (Fig. S9†), frequency sweep curves (Fig. S10†) and stress–relaxation curves (Fig. S11†) show that EGDE–MDA–BDDA also had good reprocessability. However, EGDE–MDA does not have reprocessibility due to the absence of dynamic covalent bonds.

The recyclability of the vitrimer was also investigated. Owing to the abundant ester groups, the ESO–MDA–BDDA chain should be disrupted and degraded in the presence of alcohol *via* transesterification (Fig. 6a). On the other hand, the resulting oligomers can be cured into thermoset again. Thus, the vitrimer has recyclability. Fig. 6b shows that ESO–MDA–BDDA completely degraded within 8 h in alkaline ethanol solution (pH 14) or 72 h in acidic ethanol solution (pH 1). However, it did not have mass loss in water regardless of pH. These results show that ESO–MDA–BDDA was stable in the natural environment, but rapidly degraded under basic or acidic conditions. The degradation product had a molecular weight of 1300 g mol^{-1} with a distribution index ($Đ$) of 5.59 (Fig. 6c), suggesting that it consists of oligomers. NMR analysis results shown in Fig. 6d and e further confirmed the successful degradation due to the methyl (m) and methylene (l) from EtOH which could be clearly observed. Besides, NMR analyses revealed the presence of various functional groups including ester bonds, hydroxyl groups, and tertiary amine groups. It is interesting that pressing such oligomers with a metallic mold at 160 °C under a pressure of 10 MPa for 4 h yielded a homogeneous film with the same T_g as that of the original ESO–MDA–BDDA sample. It is known that most recycled vitrimers cannot be directly cured into thermosets upon heating, and newly introduced comonomers have to be used to copolymerize with them for this purpose. Apparently, the present vitri-

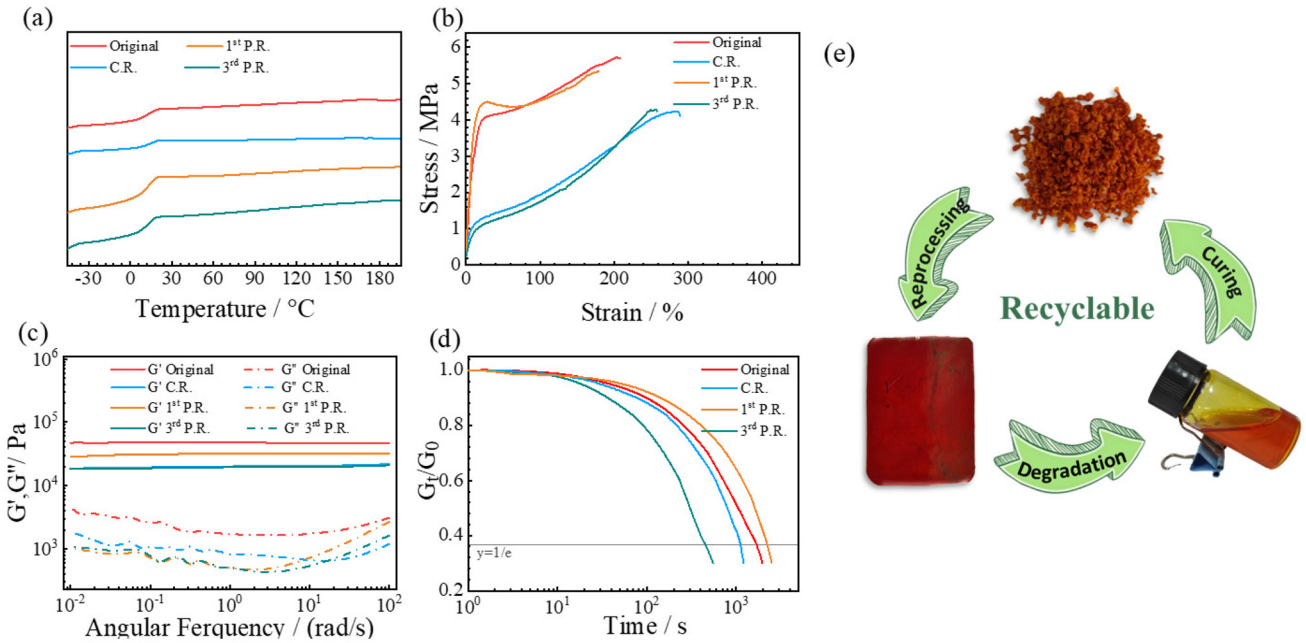

Fig. 5 (a) DSC curves; (b) stress–strain curves; (c) frequency sweep curves at 180 °C; (e) normalized stress–relaxation curves of ESO–MDA–BDDA after three cycles of repressing (1st P. R. and 3rd P. R.) or from chemical recycling (C. R.); (e) recovery process of vitrimer ESO–MDA–BDDA: 1. Reprocessed by hot-pressing at 160 °C, 10 MPa, 2 h. 2. Degradation in ethanol (pH = 14), 30 °C, 8 h; 3. After evaporation of EtOH, reprocessed by hot-pressing at 160 °C, 10 MPa, 4 h.

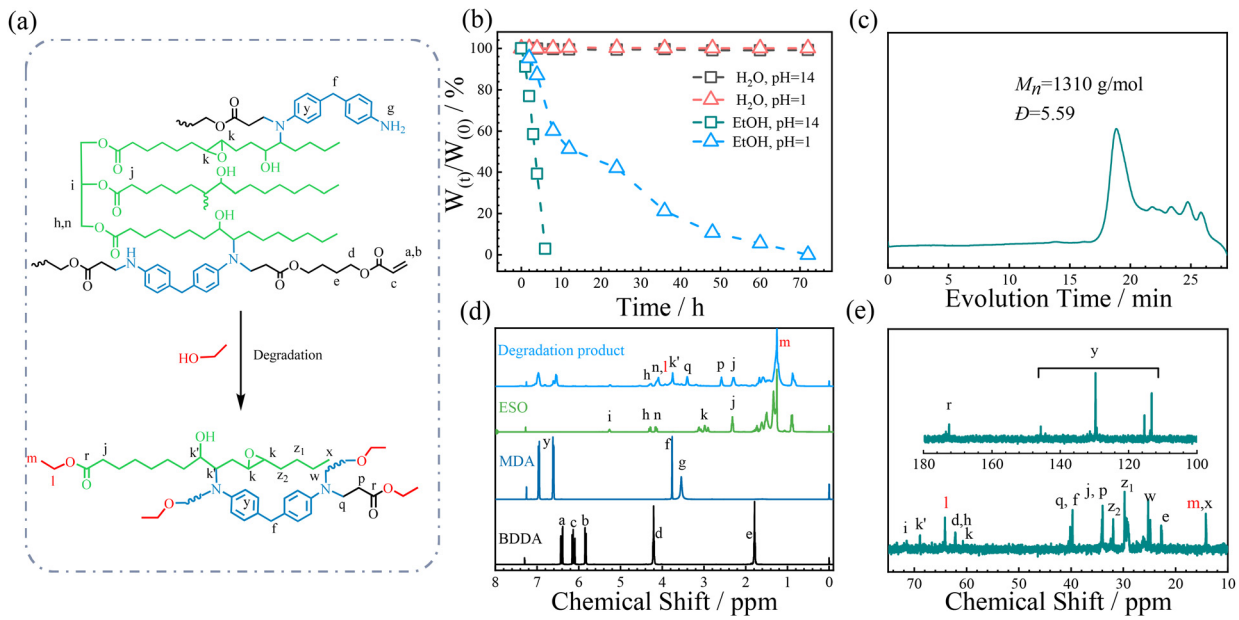

Fig. 6 (a) Degradation of ESO–MDA–BDDA; (b) weight loss ratio of ESO–MDA–BDDA at different times with different solvents and pH values; (c) GPC curve of the degraded sample; (d) ^{1}H NMR spectra of the degraded sample and the corresponding monomers for ESO–MDA–BDDA; and (e) ^{13}C NMR spectrum of the degraded sample.

mer has good recycling efficiency under mild conditions. With ester groups, EGDE–MDA–BDDA also displayed good degradability (Fig. S12†). Yet, EGDE-DMA without ester groups did not degrade (Fig. S13†).

Shape programming

The programmable shape transition of a two-dimensional sheet to a three-dimensional structure in response to various

external stimuli has attracted much attention in recent years. However, conventional epoxy vitrimers can only fix a single temporary shape under appropriate thermal treatment, enabling incomplete fabrication of a complex shape. Using the synthesis strategy here, we can readily prepare vitrimers with different stimuli-responses. That is, multi-stimuli responsible materials can be designed and programmed *via* attachment–heating of the two vitrimers. Moreover, due to the dynamic covalent bonds in the vitrimers, the adhesion between two multilayers should be strong, making sure that the shape-programmed materials have good dimensional stability. As shown in Fig. 7a, a vitrimer bilayer was fabricated by heating the two vitrimers with different T_g values. It was programmed as follows: (1) heating the vitrimer bilayer to a temperature above the T_gs of the two vitrimers and programming a temporary shape by stretching the sample with different forces. (2) Cooling down to 0 °C to fix the temporary shape by which the energy applied by stretching was stored in the vitrimer bilayer. (3) Further heating the sample to a temperature between the T_gs of the two vitrimers. At this moment, vitrimer-A with a lower T_g tended to recover its initial shape. On the other hand, vitrimer-B with the higher T_g tended to hold its existing shape. As a result, a programmed shape was achieved. That is, the shape of the samples can be programmed by tuning the extension ratio (λ). (4) On further heating the sample to a temperature above the T_g of vitrimer-B, the chains of both vitrimers start to move and the inhomogeneous internal stress in the two layers would disappear. Finally, the vitrimer bilayer returned to its initial shape.

ESO–MDA–BDDA with a T_g of 13 °C and EGDE–MDA–BDDA with a T_g of 53 °C were attached and heated at 160 °C for 4 h. During this procedure, the chains of the vitrimers diffused and interacted with each other, and the two vitrimers bonded together. This was confirmed by the SEM images of the fracture surface (Fig. S14†). Fig. 7b shows its programmed shapes. For example, the vitrimer bilayer was stretched 1.5 times its original length at 55 °C, quickly cooled to fix the shape, and then heated to 30 °C again, yielding a "U" shape. When the stretching was increased, o- and star-shaped deformations were achieved. The deformations can be completely recovered by heating the vitrimer bilayer to 55 °C. Moreover, we can further program the shape by attaching ESO–MDA–BDDA pieces onto different positions of EGDE–MDA–BDDA, so the bending of the bilayer can be controlled. As shown in Fig. 7c, four ESO–MDA–BDDA sheets with different shapes were attached to the corresponding EGDE–MDA–BDDA sheets. The letter "CCZU" was fixed after deformation, which quickly recovered at a temperature above 55 °C.

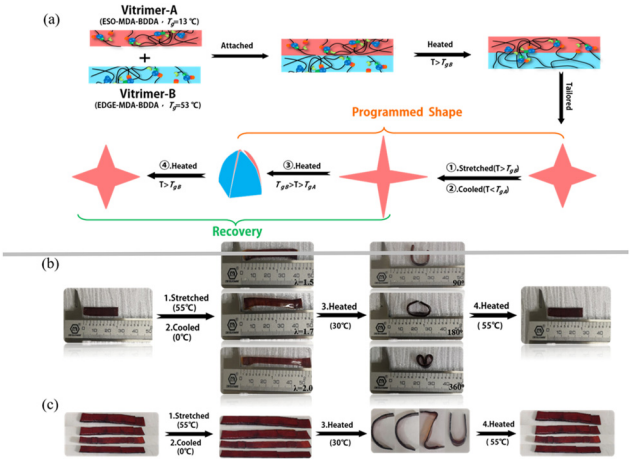

Fig. 7 (a) Programmed shape modes and recovery of the vitrimer bilayer. (b) Deformation of the vitrimer bilayer at different tensile ratios (λ); and (c) vitrimer bilayer strips for presenting the form "CCZU".

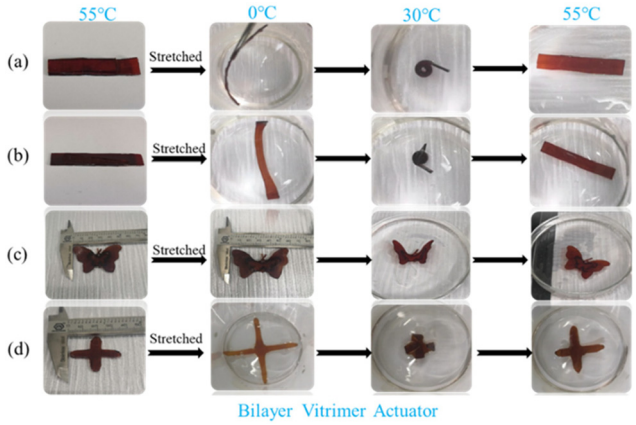

Fig. 8 Vitrimer bilayer actuators. (a) Actuating vitrimer bilayer strips to form digit "6"; (b) blooming of the flowers; (c) flapping butterfly wings; and (d) grasp and open action of the claw-shaped actuator.

Conclusion

We have synthesized recyclable and shape programmable epoxy vitrimers *via* a one-pot catalyst-free procedure by introducing diacrylate into the amine-curing bio-based epoxy. The epoxy vitrimer network possesses ester groups, β-amino esters groups, and tertiary amine groups, so it has excellent relaxation and reprocessing ability. The epoxy vitrimer can quickly degrade to oligomers in alkaline or acidic solutions. The degraded oligomers can be cured into epoxy vitrimers without the addition of new monomers. Such two vitrimers with different glass transition temperatures can be compressed into a bilayer. The bilayer can be designed and processed into a series of soft actuators to perform complex actions. The study provides a facile strategy to prepare reprocessable epoxy vitrimers which can find application in intelligent engineering.

Experimental

Materials

Epoxidized soybean oil (ESO, AR, epoxy value = 6.121), hexylamine (HA, 99%), tetrahydrofuran (THF, AR), methanol (MeOH, AR), and *n*-hexane (AR) were all from Energy Chemical. 1,4-Butanediol diacrylate (BDDA, 80%), 4,4′-methylenedianiline (MDA, 99%), ethylene glycol diglycidyl ether (EGDE, 99%), benzyl glycidyl ether (BGE, 99%), and methyl acrylate (MA, 98%) were from Aladdin. All of them were used without further purification.

Measurements

The structure of the sample was characterized by using an FTIR spectrometer (Nicolet-670) and a Bruker ARX-500 type NMR spectrometer with deuterated DMSO as the solvent and tetramethylsilane (TMS) as the internal standard at 25 °C. The thermal stability was measured using a thermogravimetric analyzer (TA SDTQ-200) in the range from room temperature to 600 °C at a heating rate of 20 °C min^{-1} under a nitrogen atmosphere. Differential scanning calorimetry (DSC) was performed using a DSC Q6000 analyzer at a nitrogen flow rate of 50 mL min^{-1}. The sample was quickly heated to 200 °C and the temperature was maintained for 10 min to remove thermal history, and then cooled to −50 °C at a rate of 10 °C min^{-1}. Afterwards, the sample was reheated to 200 °C at the same rate.

The tensile test was performed using a WDT-10 electronic universal testing tensile machine at room temperature following the ASTM D412 test standard. Frequency sweep experiments were performed using Anton Paar MCR 301 under a frequency of 1 Hz, constant force of 10 N, and variable shear strain ramped from 0.01% to 100%. Stress relaxation tests were performed using Anton Paar MCR 301 in the linear viscoelastic region at different temperatures (120 °C, 140 °C, 160 °C, 180 °C, and 200 °C) at a constant strain of 5%. Then, the changing trend of the model as a function of time was recorded. The activation energy (E_a) of stress relaxation was calculated according to the Maxwell model between relaxation time and temperature. Creep experiments at different temperatures (80–160 °C) were also carried out using Anton Paar MCR 301 and an applied force of 5 N. A 3000 Pa shear stress was applied for 300 s, and the shear strain was monitored. The reprocessing experiments were performed using a hot-pressing machine (Yan Zheng Instrument Co., Ltd, China). The sample was chopped into small pieces and then hot-pressed at 140 – 180 °C for 2–6 h with a constant pressure of 10 MPa. It was cooled to room temperature and released from the press. The microstructures of the vitrimer bilayer and the interface of two layers were observed using field emission SEM (FE-SEM, Merlin Compact, Zeiss) with an FE scanning electron microanalyzer (FEI Quanta 250, 15 kV). The vitrimer bilayer was frozen in liquid nitrogen and then fractured. A thin layer of gold was coated on the sample before SEM analysis.

Synthesis of bio-based epoxy

A typical procedure to synthesize the bio-based epoxy vitrimer is as follows. ESO (5.00 g), MDA (3.05 g), and BDDA (3.04 g) were inserted into a round-bottom flask equipped with a magnetic stirrer and stirred for 2 h at 160 °C. The homogeneous mixture was poured into a Teflon mold and cured at 160 °C for another 2 h to prepare crosslinked epoxy resin. The product was named ESO–MDA–BDDA. Other epoxy resins were prepared with the same procedure. The products were named ESO–MDA, EGDE–MDA–BDDA, and EGDE–MDA, respectively (Table 1).

Swelling ratio and gel content

The swelling ratio and gel content of the crosslinked networks were estimated by immersing the dry sample in THF, EtOH, *n*-hexane, H_2O, and DMSO for 24 h. After heating the sample for 24 h at 100 °C, the gel content and swelling ratio were calculated based on the following equations:

$$\text{Swelling ratio} = \frac{m_1 - m_0}{m_0} \times 100\% \quad (1)$$

$$\text{Gel content} = \frac{m_2}{m_0} \times 100\% \quad (2)$$

where m_0 is the original weight of the sample and m_1 and m_2 are the weights of the sample before and after swelling, respectively. The final swelling ratio and gel content for each sample are the average of three tests.

Degradation experiments

Degradation experiments were conducted by soaking a certain amount of polymer in an aqueous solution (pH 1 and 14) and an EtOH solution (pH 1 and 14). At set intervals, the polymer was removed, rinsed with deionized water three times, dried, and weighed for obtaining the mass of the residual polymers.

Programmed deformation

An ESO–MDA–BDDA or EDGE–MDA–BDDA film was cut to the designed pattern and attached firmly and subsequently heated in an oven at 160 °C for 4 h. The resulting sample was heated at 55 °C and stretched, followed by the rapid cooling of the sample to 0 °C to fix the shape. The sample was then put into the water bath at different temperatures to trigger different deformations.

Data availability

The data supporting this article have been included as part of the ESI.†

Conflicts of interest

There are no conflicts to declare.

Acknowledgements

The financial support from the National Natural Science Foundation of China (52473001&U2241286) and Priority

Academic Program Development of Jiangsu Higher Education Institutions (PAPD) is acknowledged.

References

1 R. de Luzuriaga, R. Martin, N. Markaide, A. Rekondo, G. Cabañero, J. Rodríguez and I. Odriozola, *Mater. Horiz.*, 2016, **3**, 241–247.
2 S. G. Davey, *Nat. Rev. Chem.*, 2023, **7**, 597–597.
3 X. Zhao, Y. Long, S. Xu, X. Liu, L. Chen and Y.-Z. Wang, *Mater. Today*, 2023, **64**, 72–97.
4 F. A. M. M. Gonçalves, M. Santos, T. Cernadas, P. Ferreira and P. Alves, *Int. Mater. Rev.*, 2021, **67**, 119–149.
5 R. Auvergne, S. Caillol, G. David, B. Boutevin and J.-P. Pascault, *Chem. Rev.*, 2013, **114**, 1082–1115.
6 B. Krishnakumar, A. Pucci, P. P. Wadgaonkar, I. Kumar, W. H. Binder and S. Rana, *Chem. Eng. J.*, 2022, **433**, 133261.
7 Y. Sun, M. Wang, Z. Wang, Y. Mao, L. Jin, K. Zhang, Y. Xia and H. Gao, *Macromolecules*, 2022, **55**, 523–534.
8 Y. Yang, Y. Xu, Y. Ji and Y. Wei, *Prog. Mater. Sci.*, 2021, **120**, 100710.
9 K. Tangthana-umrung, Q. A. Poutrel and M. Gresil, *Macromolecules*, 2021, **54**, 8393–8406.
10 K. S. K. Reddy, W.-J. Gao, C.-H. Chen, T.-Y. Juang, M. M. Abu-Omar and C.-H. Lin, *ACS Sustainable Chem. Eng.*, 2021, **9**, 5304–5314.
11 Y. Liu, S. Ma, Q. Li, S. Wang, K. Huang, X. Xu, B. Wang and J. Zhu, *Eur. Polym. J.*, 2020, **135**, 109881.
12 N. Zheng, Y. Xu, Q. Zhao and T. Xie, *Chem. Rev.*, 2021, **121**, 1716–1745.
13 S. Huang, X. Kong, Y. Xiong, X. Zhang, H. Chen, W. Jiang, Y. Niu, W. Xu and C. Ren, *Eur. Polym. J.*, 2020, **141**, 110094.
14 Y.-Y. Liu, G.-L. Liu, Y.-D. Li, Y. Weng and J.-B. Zeng, *ACS Sustainable Chem. Eng.*, 2021, **9**, 4638–4647.
15 G. Li, P. Zhang, S. Huo, Y. Fu, L. Chen, Y. Wu, Y. Zhang, M. Chen, X. Zhao and P. Song, *ACS Sustainable Chem. Eng.*, 2021, **9**, 2580–2590.
16 S. Huang, X. Kong, Y. Xiong, X. Zhang, H. Chen, W. Jiang, Y. Niu, W. Xu and C. Ren, *Eur. Polym. J.*, 2020, **141**, 110094.
17 S. Shan, D. Mai, Y. Lin and A. Zhang, *ACS Appl. Polym. Mater.*, 2021, **3**, 5115–5124.
18 X. Wu, P. Hartmann, D. Berne, M. De. Bruyn, F. Cuminet, Z. Wang, M. Zechner, A. D. Boese, S. V. Placet, S. Caillol and K. Barta, *Science*, 2024, **384**, 6692.
19 D. Montarnal, M. Capelot, F. Tournilhac and L. Leibler, *Science*, 2011, **334**, 965–968.
20 S. Zhao, D. Wang and T. P. Russell, *ACS Sustainable Chem. Eng.*, 2021, **9**, 11091–11099.
21 X. Yang, S. Wang, X. Liu, Z. Huang, X. Huang, X. Xu, H. Liu, D. Wang and S. Shang, *Green Chem.*, 2021, **23**, 6349–6355.
22 I. Azcune, A. Huegun, A. Ruiz de Luzuriaga, E. Saiz and A. Rekondo, *Eur. Polym. J.*, 2021, **148**, 110362.
23 H. Si, L. Zhou, Y. Wu, L. Song, M. Kang, X. Zhao and M. Chen, *Composites, Part B*, 2020, **199**, 108278.
24 X. Xu, S. Ma, S. Wang, J. Wu, Q. Li, N. Lu, Y. Liu, J. Yang, J. Feng and J. Zhu, *J. Mater. Chem. A*, 2020, **8**, 11261–11274.
25 H. Liu, H. Zhang, H. Wang, X. Huang, G. Huang and J. Wu, *Chem. Eng. J.*, 2019, **368**, 61–70.
26 H. Memon, H. Liu, M. A. Rashid, L. Chen, Q. Jiang, L. Zhang, Y. Wei, W. Liu and Y. Qiu, *Macromolecules*, 2020, **53**, 621–630.
27 X. Fang, N. Tian, W. Hu, Y. Qing, H. Wang, X. Gao, Y. Qin and J. Sun, *Adv. Funct. Mater.*, 2022, **32**, 2208623.
28 Y. Xiao, P. Liu, W. Wang and B. Li, *Macromolecules*, 2021, **54**, 10381–10387.
29 B. Marco-Dufort, R. Iten and M. W. Tibbitt, *J. Am. Chem. Soc.*, 2020, **142**, 15371–15385.
30 Y. Zeng, S. Liu, X. Xu, Y. Chen and F. Zhang, *Polymer*, 2020, **211**, 123116.
31 X. Zhang, S. Zhang, W. Liu, Y. Abbas, Z. Wu, Y. Eichen and J. Zhao, *Chem. Eng. J.*, 2021, **411**, 128467.
32 L. M. Sridhar, M. O. Oster, D. E. Herr, J. B. D. Gregg, J. A. Wilson and A. T. Slark, *Green Chem.*, 2020, **22**, 8669–8679.
33 S. Wang, S. Ma, J. Qiu, A. Tian, Q. Li, X. Xu, B. Wang, N. Lu, Y. Liu and J. Zhu, *Green Chem.*, 2021, **23**, 2931–2937.
34 M. Hayashi and R. Yano, *Macromolecules*, 2019, **53**, 182–189.
35 B. Xue, R. Tang, D. Xue, Y. Guan, Y. Sun, W. Zhao, J. Tan and X. Li, *Ind. Crops Prod.*, 2021, **168**, 113583.
36 S. Wang, J. Dai, N. Teng, J. Hu, W. Zhao and X. Liu, *ACS Sustainable Chem. Eng.*, 2020, **8**, 16842–16852.
37 Y. Liu, B. Wang, S. Ma, T. Yu, X. Xu, Q. Li, S. Wang, Y. Han, Z. Yu and J. Zhu, *Composites, Part B*, 2021, **211**, 108654.
38 J. Zhang, Z. Gong, C. Wu, T. Li, Y. Tang, J. Wu, C. Jiang, M. Miao and D. Zhang, *Green Chem.*, 2022, **24**, 6900–6911.
39 J. Wu, X. Yu, H. Zhang, J. Guo, J. Hu and M. Li, *ACS Sustainable Chem. Eng.*, 2020, **8**, 6479–6487.
40 J. Wu, L. Gao, Z. Guo, H. Zhang, B. Zhang, J. Hu and M. Li, *Green Chem.*, 2021, **23**, 5647–5655.
41 Y. Tao, L. Fang, M. Dai, C. Wang, J. Sun and Q. Fang, *Polym. Chem.*, 2020, **11**, 4500–4506.
42 A. A. Putnam-Neeb, A. Stafford, S. Babu, S. J. Chapman, C. M. Hemmingsen, M. S. Islam, A. K. Roy, J. A. Kalow, V. Varshney, D. Nepal and L. A. Baldwin, *ACS Appl. Polym. Mater.*, 2024, DOI: **10.1021/acsapm.3c03082**.
43 D. Berne, F. Cuminet, S. Lemouzy, C. Joly-Duhamel, R. Poli, S. Caillol, E. Leclerc and V. Ladmiral, *Macromolecules*, 2022, **55**, 1669–1679.
44 Y. R. Zhang, S. Gu, Y. Z. Wang and L. Chen, *Sustainable Mater. Technol.*, 2024, **40**, e00883.
45 W. Li, L. Xiao, J. Huang, Y. Wang, X. Nie and J. Chen, *Sci. Technol.*, 2022, **227**, 109575.
46 S. Guggari, F. Magliozzi, S. Malburet, A. Graillot, M. Destarac and M. Guerre, *Polym. Chem.*, 2024, **15**, 1347–1357.
47 H. X. Niu, T. M. Yang, X. Wang, P. Zhang, W. Guo, L. Song and Y. Hu, *Green Chem.*, 2024, **26**, 5519.
48 A. Kumar and L. A. Connal, *Rapid Commun.*, 2023, **44**, 2200892.

49 L. Zhong, Y. Hao, J. Zhang, F. Wei, T. Li, M. Miao and D. Zhang, *Macromolecules*, 2022, **55**, 595–607.
50 A. Roig, X. Ramis, S. D. Flor and A. Serra, *Eur. Polym. J.*, 2024, **206**, 112782.
51 H. J. Yang, Z. Y. Ren, Y. K. Zuo, Y. Y. Song, L. Jiang, Q. M. Jiang, X. Q. Xue, W. Y. Huang, K. J. Wang and B. B. Jiang, *ACS Appl. Mater. Interfaces*, 2020, **12**, 50870–50878.
52 H. J. Yang, J. D. Zhang, Y. Y. Song, L. Jiang, Q. M. Jiang, X. Q. Xue, W. Y. Huang and B. B. Jiang, *Macromol. Chem. Phys.*, 2020, **222**, 2000263.
53 H. J. Yang, H. X. Yao, K. F. Feng and G. Z. Zhang, *Polymer*, 2022, **260**, 125340.
54 C. Taplan, M. Guerre and F. E. Du Prez, *J. Am. Chem. Soc.*, 2021, **143**, 9140–9150.